LIMNOLOGY and OCEANOGRAPHY

ASLO

Limnol. Oceanogr. 9999, 2020, 1–17

doi: 10.1002/lno.11602

Phosphorus dynamics in the Barents Sea

Patrick P. Downes,[1,2] **Stephen J. Goult**,[1] **E. Malcolm S. Woodward**,[1] **Claire E. Widdicombe**,[1] **Karen Tait**,[1] **Joanna L. Dixon**[1*]

[1]Plymouth Marine Laboratory, Plymouth, UK
[2]University of Bristol, Bristol, UK

Abstract

The Barents Sea is considered a warming hotspot in the Arctic; elevated sea surface temperatures have been accompanied with increased inflow of Atlantic water onto the shelf sea. Such hydrodynamic changes and a concomitant reduction of sea ice coverage enables a prolonged phytoplankton growing season, which will inevitably affect nutrient stoichiometry and the controls on primary production. During the summer of 2018, we investigated the role of phosphorus in mediating primary production in the Barents Sea. Dissolved inorganic phosphorus (DIP), its most bioavailable form, had an average net turnover time of 9.4 ± 4.8 d. The most southern Atlantic influenced station accounted for both the highest rates of primary production (655 mg C m^2 d^{-1}) and shortest net DIP turnover (2.8 ± 0.5 d). The fraction of assimilated DIP released as dissolved organic phosphorus (DOP) at this station was < 4% compared to an average of 21% at all other stations. We observed significant differences between phytoplankton communities in Arctic and Atlantic waters within the Barents Sea. Slower DIP turnover and greater release of DOP was associated with *Phaeocystis pouchetii* dominated communities in Arctic waters. Faster turnover rates and greater phosphorus retention occurred among the Atlantic phytoplankton communities dominated by *Emiliania huxleyi*. These findings provide baseline measurements of P utilization in the Barents Sea, and suggest increased Atlantic intrusion of this region could be accompanied by more rapid DIP turnover, possibly leading to future P limitation (rather than N limitation) on primary production.

Phosphorus (P) uptake by oceanic plankton has received little attention compared to nitrogen (N), mainly because N is considered limiting over biologically relevant time scales, and P over geological time scales (Hecky and Kilham 1988; Tyrrell 1999). Despite this, evidence is mounting to suggest P can be the proximal limiting macronutrient for primary production in various marine environments, particularly warm oligotrophic systems and coastal waters with enhanced N enrichment (Bjorkman and Karl 1994; Wu et al. 2000; Thingstad et al. 2005). While global primary production is expected to decrease as a result of warmer temperatures enhancing water column stratification (Falkowski et al. 1998; Behrenfeld et al. 2006), the Arctic is expected to see an increase in production due to reduced light limitation caused by declining sea ice extent and thickness (Carmack et al. 2006). Extended areas of open water in Arctic systems could additionally lead to longer periods of phytoplankton growth and resulting nutrient limitation (Tremblay and Gagnon 2009). Thus, baseline knowledge of microbial P dynamics in Arctic waters is necessary to understand future productivity and associated changes in this region.

DIP is the most readily available form of P for phytoplankton; this pool is largely comprised of phosphate (PO_4). When PO_4 is depleted in the euphotic zone relative to other nutrients, primary production becomes P limited. Such conditions generally favor smaller phytoplankton species with a high surface area to volume ratio, as cellular P quotas and uptake rates scale with cell size (Edwards et al. 2012; Lomas et al. 2014). Hence, it has been widely reported that the smaller size fraction of the plankton community (< 3 μm) contribute to the majority of P uptake fluxes (Bjorkman and Karl 1994; Thingstad et al. 1998; Moutin et al. 2002; Tanaka et al. 2003). The availability of PO_4 can therefore impact the biological carbon pump, both in regulating the magnitude of primary production and influencing species composition, whereby low PO_4 conditions relative to other nutrients can favor smaller phytoplankton species with slower sinking velocities.

An alternative source of P for phytoplankton is in the form of dissolved organic phosphorus (DOP). The proportion of

*Correspondence: jod@pml.ac.uk

Special Issue: Biogeochemistry and Ecology across Arctic Aquatic Ecosystems in the Face of Change
Edited by: Peter J. Hernes, Suzanne Tank and Ronnie N. Glud

DOP in the total dissolved P pool varies regionally. For example, in shelf seas DOP accounts for 11–86% of the total dissolved P in the photic zone, this proportion is often greater in oligotrophic open ocean systems, ranging between ~ 66% and 100% (Karl and Björkman 2015 and references therein). The chemical composition of DOP dictates its availability for biological assimilation. However, the chemical form and thus bioavailability of DOP is mostly unknown (Karl 2014). DOP originates from organic matter production with subsequent release via exudation, grazing, or cell lysis (Karl and Björkman 2015). Advective transport of DOP can provide downstream regions with an additional P source, and it has been postulated that this could be the case for Atlantic water entering the Barents Sea shelf (Torres-Valdes et al. 2009).

In order to utilize DOP which is not readily available for assimilation, microbes hydrolyse P from the organic moiety prior to uptake, and this is usually induced by the ectoenzyme alkaline phosphatase (AP). Thus, enhanced AP activity can be a proxy for DIP limitation (Rees et al. 2009; Lomas et al. 2010; Mahaffey et al. 2014; Labry et al. 2016). However, elevated AP activity has also been reported in DIP-replete conditions (Sebastian et al. 2004; Labry et al. 2016; Davis and Mahaffey 2017). Such ambiguity highlights the need for multiple, simultaneous indicators when investigating microbial P dynamics, including net and gross turnover time of phosphorus pools. Net turnover accounts for the fraction of DIP assimilated into the particulate fraction, while gross turnover includes the uptake of DIP and release of DOP. The difference between net and gross turnover gives an estimation of P retention. Low DOP release (high retention) and efficient recycling of P due to low ambient DIP concentrations has been demonstrated in Celtic Sea post spring phytoplankton bloom scenarios (Poulton et al. 2019).

The Barents Sea is a highly productive shelf sea experiencing seasonal ice cover. This region acts as a gateway between the Arctic and Atlantic Ocean, with an inflow of warmer saline Atlantic water from the south and colder fresher Arctic waters dominating the Northern region (Loeng et al. 1997). Over the past 30 yrs, the volume of Atlantic water entering the shelf sea has doubled (Oziel et al. 2016), while sea ice import has declined (Lind et al. 2018). This loss of freshwater and intrusion of saline Atlantic water has led to reduced sea ice formation (Lind et al. 2018). The Barents Sea accounts for approximately 40% of Arctic shelf sea primary production (PP) (Arrigo and van Dijken 2015). Ice algae account for ~ 6% of annual PP in the region, with the majority being associated with pelagic phytoplankton (Wassmann et al. 2006). During spring, the seasonal ice zone retreats giving way to open water with a marginal ice zone on the boundary, this is accompanied by a northward progressing spring bloom (Sakshaug and Skjoldal 1989). The phytoplankton blooms succeeding the ice retreat are characterized by eutrophic conditions and new production, this is then followed by an oligotrophic summer period (Luchetta et al. 2000), during which nitrate is depleted to greater extent relative to DIP and silicate, and regenerated nutrients sustain phytoplankton growth (Erga et al. 2014).

Phytoplankton assemblages in the Barents Sea have been extensively studied, especially around the polar front, which is generally dominated by diatoms and the prymnesiophyte *Phaeocystis pouchetii* (Sakshaug et al. 1994; Wassmann et al. 1999; Degerlund and Eilertsen 2010). Observations in recent years, both in situ and satellite, have reported trends of extensive blooms of the coccolithophore *Emiliania huxleyi* (Smyth et al. 2004; Hegseth and Sundfjord 2008; Erga et al. 2014; Hovland et al. 2014; Oziel et al. 2017), a calcifying species typically associated with warmer temperate waters. *E. huxleyi* is known to occupy a niche of low nutrient conditions and increased stratification post spring bloom (Tyrrell and Merico 2004; Lessard et al. 2005). With rising temperatures and increased "Atlantification," *E. huxleyi* blooms are expected to increase in the Barents Sea in the future (Neukermans et al. 2018).

To our knowledge, there are no extensive studies of P uptake in the Arctic shelf marine environments. Therefore, the aim of this work was to build an understanding of P utilization in the Barents Sea, during the summer growing season where phytoplankton growth can be nutrient limited. We provide measurements of DIP uptake, DOP release and AP activity across a spatial gradient covering Atlantic and Arctic waters.

Materials and methods

Study area and sampling

Experiments were conducted at six stations in the Barents Sea aboard the *RRS James Clark Ross* (JR17007), between the 11th and 29th July 2018, as part of the UK Changing Arctic Ocean Seafloor programme (ChAOS; Fig. 1). Depth profiles of temperature and salinity were determined using a SEA-BIRD CTD system mounted on a rosette sampler equipped with 24 Niskin bottles (20 L) to collect seawater at defined depths. At each station, six light depths were sampled corresponding to set photosynthetically active radiation (PAR) percentages (100%, 50%, 25%, 15%, 3%, 1%), calculated from the surface PAR (log). Samples were collected in 2 L polycarbonate bottles before immediate subsampling and processing as described below.

Inorganic nutrients and P*

Samples for nutrient analysis were collected and immediately stored at − 20°C, before returning to Plymouth Marine Laboratory for analysis. Dissolved inorganic nitrogen (DIN) is defined as the combined concentration of inorganic nitrate and nitrite, while DIP is assumed to be the concentration of soluble reactive phosphorus (Thomson-Bulldis and Karl 1998). Ambient DIN, DIP, and silicate concentrations were

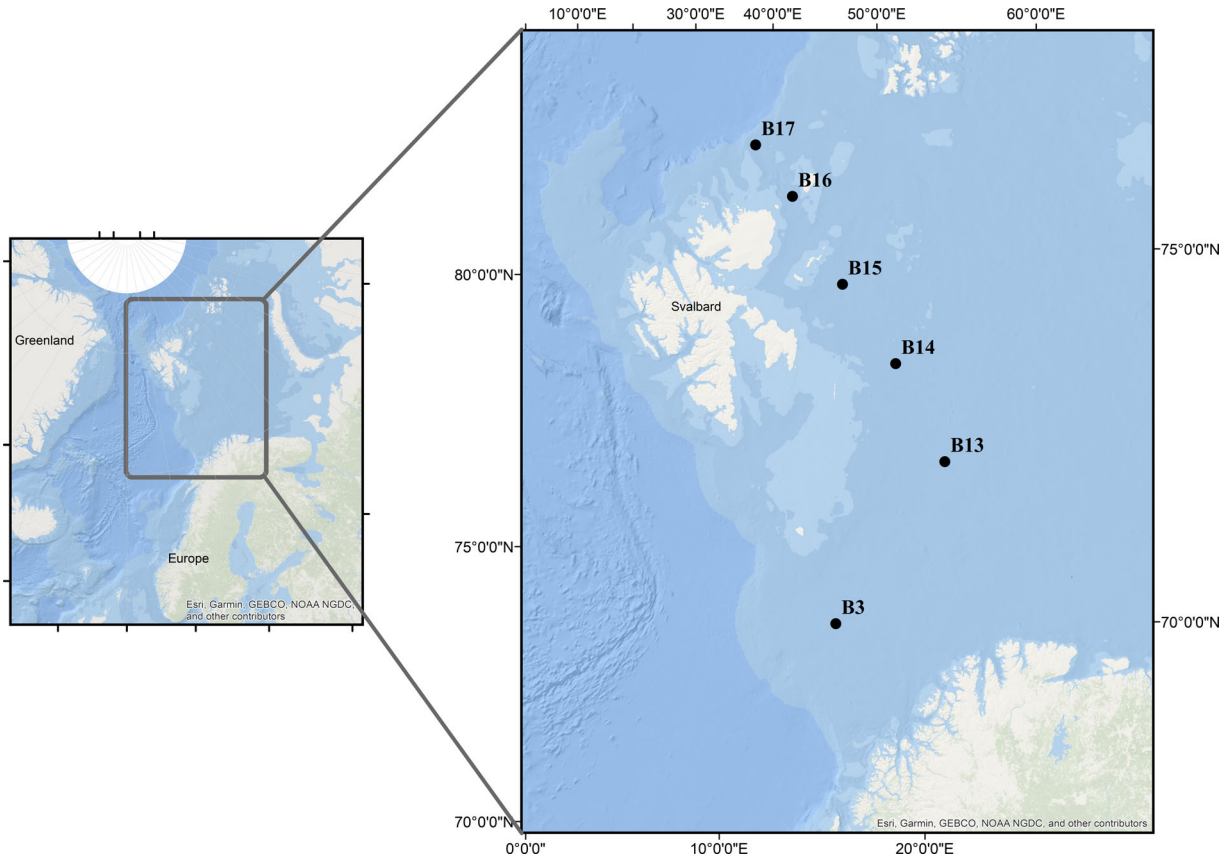

Fig 1. Stations sampled during the Changing Arctic Ocean Seafloor cruise (JR17007).

determined using a SEAL analytical AutoAnalyzer II, segmented flow colorimetric autoanalyzer, in accordance with the protocols outlined in Woodward and Rees (2001). To assess deviations of DIN : DIP ratios from the Redfield ratio, P* was calculated (Deutsch and Weber 2012):

$$P^* = DIP - (DIN/16)$$

Dissolved organic phosphorus

Ambient DOP concentrations were estimated as the difference between total dissolved phosphorus (TDP) and DIP. To measure TDP the persulfate oxidation method was used to liberate organically bound P, before measuring DIP (Menzel and Corwin 1965; Ridal and Moore 1990). After collection at sea samples were stored in polycarbonate bottles at – 20°C. Before analysis, samples were thawed and filtered (0.22 μm pore size, Millipore) into glass vials with PTFE lined caps for the oxidation step (Yoshimura 2013). Briefly, potassium persulfate solution was added to 20 mL acidified sample, 0.8% final concentration, and autoclaved for 2 h at 123°C. Samples were placed in a water bath at 90°C for 2 h to remove excess chlorine before measuring DIP. Triplicate measurements on select samples gave an approximate precision of ± 1%.

Dissolved inorganic phosphorus uptake and release of dissolved organic phosphorus

Daily rates of DIP uptake were determined using ^{33}P tracer experiments (Canellas et al. 2000). Water samples were aliquoted into 60 mL acid washed polycarbonate bottles (3 light, 1 dark). Each bottle was spiked with 5–12 kBq ^{33}P-orthophosphoric acid (Perkin Elmer, specific activity 5–7 kBq pmol^{-1}) equating to an addition of < 3 pmol DIP. Bottles were then placed in on-deck incubators with light density filters corresponding to the PAR depths sampled. Incubations were carried out for 24 h, and temperature was maintained by a continuous supply of surface seawater. The contents of the bottles were filtered onto 47 mm diameter 0.2 μm polycarbonate filters presoaked and boiled in a lithium chloride phosphate buffer (1 mM PO_4); which prevents unincorporated $^{33}PO_4$ adsorbing to filter surfaces. Filters were counted using a liquid scintillation counter (TriCarb 3100TR) using ProSafe FC+ liquid scintillation cocktail (Meridian Biotechnologies Ltd).

The release of DOP from cells was determined following Poulton et al. (2019). Before filtration at the end of the incubation, 10 mL aliquots were removed from incubation bottles at four light depths per station. The aliquot was filtered using a 25 mm diameter 0.2 μm polycarbonate filter (Millipore ™) and the filtrate collected in 20 mL glass vials. The filtrate was then

transferred into 15 mL centrifuge tubes, with the addition of 250 μL NaOH solution (1 M) (Thomson-Bulldis and Karl 1998; Bjorkman et al. 2000; Poulton et al. 2019), vortexed, and then centrifuged at 3500 rpm for 1 h. To measure the ^{33}P-DOP, 1 mL of the supernatant was placed in a 20 mL glass scintillation vial with 8 mL ProSafe HC+ liquid scintillation cocktail (Meridian Biotechnologies Ltd) prior to counting. The estimate of ^{33}P-DOP should be considered a minimum due to a possible loss by coprecipitation with NaOH.

To estimate the percentage of assimilated DIP released as DOP, the gross rate of DIP uptake was calculated (i.e., the rate of DIP uptake plus the rate of DOP production). The percentage release of DOP was therefore the fraction of gross DIP uptake measured as DOP release multiplied by 100. Gross and net turnover times were calculated accordingly.

AP activity

AP activity was measured fluorometrically with the substrate 4-MUF-phosphate (Hoppe 1983). The fluorogenic substrate was dissolved to a final concentration of 10 mM in 50% dimethyl sulfoxide. For each depth sampled, triplicate 3 mL aliquots were dispensed into 5 mL cuvettes and amended with a final concentration of 150 μM MUF-phosphate. Incubations were carried out in the dark at in situ temperatures. Fluorescence measurements were taken immediately after substrate addition and at 3–4 time points up to 24 h using a Turner biosystems TBS solid-state fluorometer using the "UV" channel (excitation 365 nm; emission 440–470 nm). Calibrations were carried out using six methylumbelliferone standards with a concentration range 2.5–100 nM L^{-1}.

Primary production

Rates of net primary production (PP) were estimated from the six light depths sampled according to Joint and Pomroy (1993). Triplicate samples were dispensed into 60 mL acid washed polycarbonate bottles, inoculated with 370 kBq (10 μCi) $NaH^{14}CO_3$ and incubated on-deck at simulated PAR depths for 24 h, simultaneous with DIP uptake experiments. Incubations were terminated by sequential filtration through 20, 2, and 0.2 μm polycarbonate filters (Millipore™). Filters were fumed with HCl (37%) for 2 h and desiccated for 12 h prior to counting using ProSafe FC+ liquid scintillation cocktail (Meridian Biotechnologies Ltd).

Phytoplankton community composition

Samples for phytoplankton enumeration were taken at four depths per station representing the surface, sub surface, chlorophyll maximum and 1% PAR depth. Duplicate samples were fixed, one with acid Lugol's solution (2% final concentration) and the other with neutral formalin (4% final concentration). Analysis was carried out using inverted settlement microscopy (Widdicombe et al. 2010), with identification to species level where possible using Lugol's fixed samples for noncalcifying species and formalin fixed samples for calcifying coccolithophores.

Satellite chlorophyll and sea ice extent

To contextualize our sampling period in terms of the summer phytoplankton growing season we used satellite chlorophyll data processed by the NERC Earth Observation Data Acquisition and Analysis Service (NEODAAS) from NASA OBPG L2 data using SeaDAS version 7.3. Chlorophyll *a* (Chl *a*) measurements were extracted from rolling 28-day 1.1 km resolution mean surface composites for each cruise station from March to October 2018, using the NASA Suomi-VIIRS Standard Chlorophyll-A Ocean Color Index algorithm. The OCI algorithm merges the color index product outlined in Hu et al. (2012) with the Ocean Chlorophyll 3 product documented in O'Reilly et al. (2000) combined using a weighted blend which provides improved coverage and accuracy.

Sea ice area fractions were extracted from the Operational Sea Surface Temperature and Sea Ice Analysis dataset (Donlon et al. 2012), provided by the "Group for High Resolution Sea Surface Temperature," the Met Office and the Copernicus Marine Environment Monitoring Service and all processed by NEODAAS. Sea ice area fractions were extracted for each cruise station from daily 5 km resolution composite data. Days that were ice free prior to sampling were calculated from the first day the station area had < 10% ice cover to the day of sampling.

Statistical analysis

One-way ANOVA was used to determine variance of environmental data and rate measurements between Atlantic and Arctic influenced stations, performed using Matlab R2018a. Multivariate patterns of phytoplankton community assemblages and their relationships to environmental variables were analyzed using the statistical package PRIMER (Clarke and Green 1988; Clarke 1993; Clarke and Ainsworth 1993). Phytoplankton abundances were square root transformed, from which a Bray–Curtis similarity matrix was generated and used to create a two-dimensional nonmetric multidimensional scaling (NMDS) ordination, to visualize multivariate patterns of phytoplankton community composition. ANOSIM (Analysis of similarity) was employed to test the significance of the NMDS. It was then analyzed for statistical correlation with several environmental variables using BEST; coupling Spearman rank correlation (BIO-ENV) with permutation analysis.

Results

Environmental parameters

The cruise transect represented a clear gradient in the Barents Sea from Atlantic water in the south to Arctic water with overlying melt water at the northern three stations (Table 1), with the polar front situated between Sta. B14 and B15. Hence, we will refer to the Atlantic region as Sta. B3, B13, and B14 and the Arctic region being Sta. B15–B17. All stations

Table 1. Station locations, water masses, sea surface temperature and days ice free prior to sampling. Depth integrated primary production measurements and dominant phytoplankton groups.

Site	Lat. (°N) long. (°E)	Surface water masses*	~Sea surface temp. (°C)	Days ice free prior to sampling	∑ primary production (mg C m^2 d^{-1})	Dominant phytoplankton
B3	72.63	AtW	9.7	N/A†	655	*Emiliania huxleyi*
	19.25					*Psuedo-nitzschia delicatissima*
						Phytoflagellates (<5 μm)
B13	74.50	AtW	6.5	N/A†	307	*Emiliania huxleyi*
	30.00					*Prorocentrum f.minimum*
B14	76.50	AtW	5.0	82	184	*Gymnodiniales*
	30.50					*Peridiniales*
B15	78.25	ArW/MW	2.6	46	118	*Phaeocystis pouchetii*
	30.00					
B16	80.11	ArW/MW	2.4	46	41.4	*Phaeocystis pouchetii*
	30.06					
B17	81.28	ArW/MW	1.7	43	605	*Phaeocystis pouchetii*
	29.32					*Thalassiosira*

*Water masses as define in Oziel et al. (2016) and Vage et al. (2016), Alantic water (AtW), Arctic water (ArW), and Melt water (MW).
†Stations were ice free all year prior to sampling.

were free of sea ice at the time of sampling; B14 was the only Atlantic influenced station to experience winter sea ice cover, but remained ice free for 82 d prior to sampling, compared to 43–46 d for the Arctic stations (Table 1).

For the Atlantic stations; DIN, DIP and silicate concentrations in the upper water column (0–50 m) followed similar latitudinal patterns with a northward gradient of decreasing surface nutrients (Fig. 2). The highest ambient concentrations were observed at Sta. B3, with DIN ranging from 4.70–7.31 μM, DIP: 0.31–0.44 μM, and silicate: 2.75–3.17 μM (Fig. 2A–C; Table 2). Compared to much lower concentrations at the northern most Atlantic Sta. B14 with DIN, DIP and silicate ranging from 0.02–0.04, 0.09–0.09, and 0.53–0.67 μM, respectively (Fig. 2A–C; Table 2). At the Arctic stations sampled nutrient concentrations varied considerably. The lowest values measured were at Sta. B16, DIN ranged between 0.04–2.86 μM and DIP between 0.08–0.32 μM, compared to much higher concentrations at Sta. B17, 0.04–6.60 and 0.10–0.88 μM, respectively (Table 2; Fig. 2A,B). Depth profiles reveal a much deeper nutricline depth for DIN and DIP at B16 opposed to B15 and B17, being more pronounced for DIN compared to DIP (Fig. 2A, B). Furthermore, at Sta. B17, high ambient DIP (0.88 μM) measured at 39 m depth corresponds with high DIN (6.6 μM) and a hotspot in DOP concentration (0.50 μM) (Fig. 2A,B,D). These high nutrient concentrations at 39 m coincided with a peak in primary productivity (Fig. 3F). With the exception of Sta. B3, silicate was depleted in the surface waters, ranging between 0.36 and 2.55 μM, including a notable hotspot in overlying melt water at B16 (Fig. 2C; Table 2). DOP generally remained higher in the surface waters and decreased with depth. Above the nutricline DOP accounted for 37–78% of the TDP pool, with no significant difference between the Atlantic and Arctic stations sampled (ANOVA, $F = 1.75$, $p < 0.19$).

Primary production, phytoplankton, and chlorophyll

Satellite surface chlorophyll estimates suggest that our sampling periods represented post bloom scenarios at all stations (Fig. 4). The spring bloom occurred in Atlantic waters during May, being more pronounced at Sta. B13 and B14 compared to B3. Bloom timing was later at the Arctic stations, occurring in June, and B17 showed a second chlorophyll peak during September. Late summer/early autumn blooms also occurred at the Atlantic stations albeit at varying timings (Fig. 4). However, satellite chlorophyll estimates typically capture the first optical depth only, and are therefore not able to account for sub surface chlorophyll peaks. The experimentally derived depth profiles show distinct subsurface peaks in PP for the three Arctic stations (Fig. 3C,D,F) compared to the Atlantic stations where PP was high at the surface and decreased with depth (Fig. 3A–C). Thus when using satellite estimates to contextualize in situ data, in terms of the timing of phytoplankton blooms, there will be greater uncertainty for the Arctic stations where more discrete nonsurface blooms will be missed. However, overall the temporal variations in surface chlorophyll demonstrate that our ship derived measurements represent summer phytoplankton growth occurring post spring bloom and before any late summer/autumn blooms.

Depth integrated primary production (Table 1; Fig. 3) estimates show the southern station (B3) accounted for the highest PP in Atlantic waters (655 mg C m^2 d^{-1}) and the

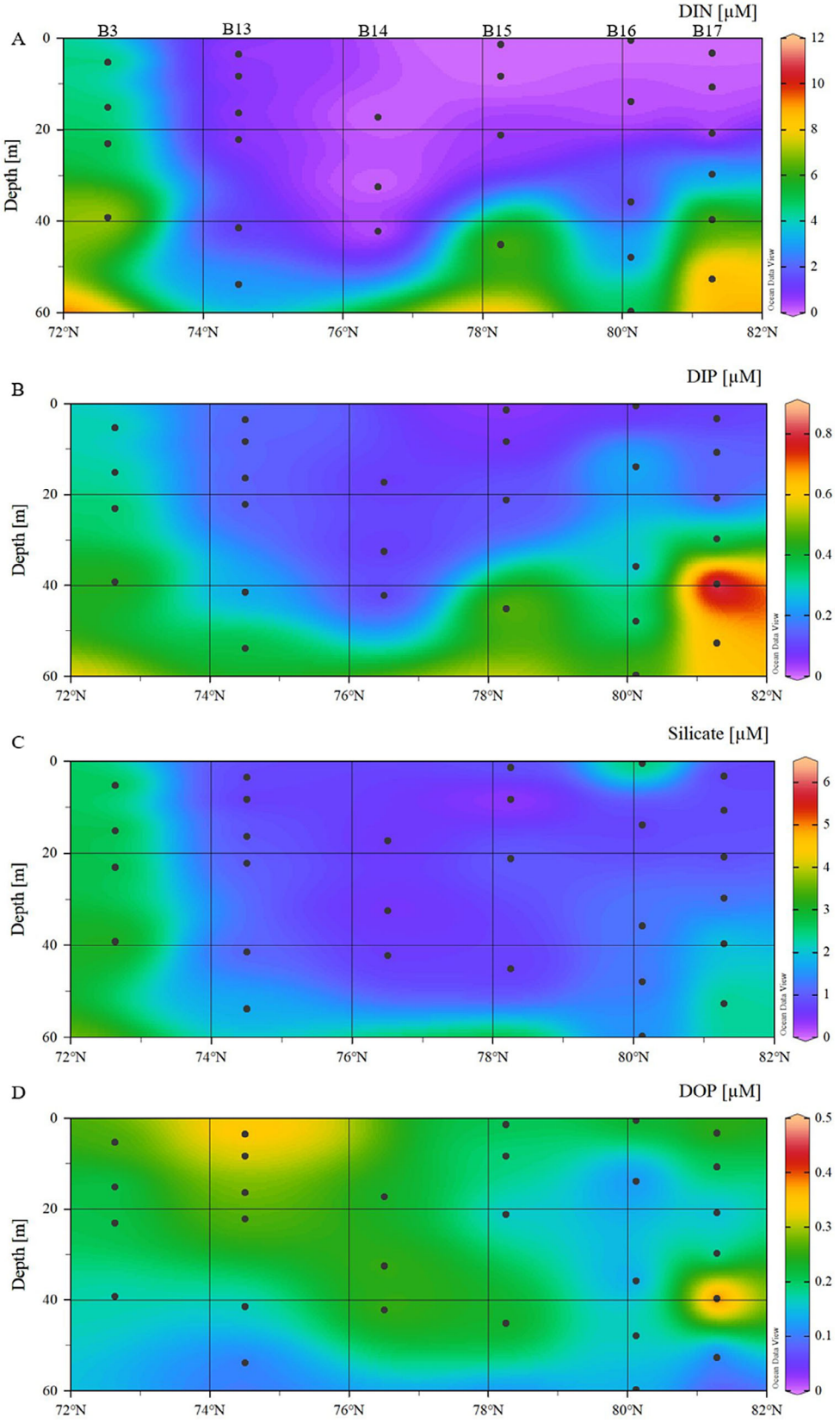

Fig 2. Section plots: (**A**) dissolved inorganic nitrogen (DIN), (**B**) dissolved inorganic phosphorus (DIP), (**C**) silicate, and (**D**) dissolved organic phosphorus (DOP).

northern most station (B17) having the highest rates in Arctic waters (605 mg C m^2 d^{-1}). Depth profiles reveal a defined subsurface peak in PP at the 15% PAR depth for the three Arctic stations (Fig. 3D–F), which occurs below the overlying melt water. The dominant phytoplankton species at these stations was *P. pouchetii* (Table 1) belonging to the nano (2–20 μm) size class, which accounted for 55–77% of PP at the Arctic stations. At Sta. B15 and B16 the subsurface peak in PP was shallower ($\sim$ 20 m) and corresponded to lower nutrient availability compared to a deeper peak in PP ($\sim$ 40 m) observed at Sta. B17, with much higher ambient DIN, DIP, and DOP concentrations (Figs. 2A–C, 3D–F). Furthermore, the magnitude of subsurface PP at B17 (27.8 ± 10.9 mg C m^{-3} d^{-1}) was considerably higher than that measured at B15 and B16, 4.33 ± 1.03 and 1.54 ± 0.50 mg C m^{-3} d^{-1}, respectively.

The stations in Atlantic waters, with no overlying melt water, were typically characterized by the highest PP in the surface, decreasing with depth. The nanosize class accounted for 76% of PP at B3, and was comprised mainly of phytoflagellates and *E. huxleyi* (Table 1). To a lesser extent B13 also had a large contribution of the nanosize class to total PP (57%), which was, similar to Sta. B3, dominated by *E. huxleyi*. Sta. B13 also had a large contribution of the micro size class (> 20 μm), accounting for 35% of PP and being comprised mainly of dinoflagellates e.g., *Prorocentrum f.minimum* (Table 1). Similarly, micro sized phytoplankton accounted for 33% of PP at B14, again being comprised mainly of dinoflagellates e.g., *Peridiniales* and *Gymnodiniales*. Overall the phytoplankton species composition showed a trend from autotrophic nanosized plankton dominating the high rates of PP at B3, with increasingly more micro sized (> 20 μm) dinoflagellates capable of mixotrophy toward B14 where nutrients were increasingly depleted. *E. huxleyi* was confined to the warmer waters (≥ 6 °C) at Sta. B3 and B13. Whereas, *P. pouchetii* was present in Arctic waters only, being the dominant species at Sta. B15–B17.

Patterns of similarity between phytoplankton species composition and abundance can be visualized with NMDS ordination (Fig. 5). Assemblages within Arctic and melt water show a defined cluster separate from the Atlantic communities, which form individual clusters according to stations. The ANOSIM model was employed to test the degree of significance of the NMDS giving a dissimilarity of 61.1% ($p < 0.008$) between the Arctic and Atlantic communities. Results from BEST analysis show the environmental variables that significantly correlated ($p < 0.02$) with the multivariate pattern of community composition across all stations (Table 3). Here silicate and temperature were in all the combinations of environmental variables correlating with patterns of species composition. We repeated the same analysis separately for the Atlantic and Arctic stations. For the three Arctic stations there was no significant correlation ($p < 0.69$), this was expected due to small differences in the species composition between Arctic stations (Fig. 5). Whereas the Atlantic stations had a significant correlation

Table 2. Inorganic nutrient concentrations: Dissolved inorganic nitrogen (DIN), silicate, dissolved inorganic phosphorus (DIP). Deviations of DIN : DIP compared Redfield ratio (P*). Dissolved organic phosphorus concentrations (DOP). Bulk activity measurements: DIP net uptake, net and gross turnover times, percentage of DIP incorporated released as DOP and alkaline phosphatase activity (APA). Mean ± standard deviation, along with minimum and maximum values observed in the surface ~ 50 m.

Sta.	DIN (μM)	Silicate (μM)	DIP (μM)	P*	DOP (μM)	DIP net uptake (nM d^{-1})	DIP net turnover time (d)	DIP gross turnover time (d)	DOP release (%)	APA (nM h^{-1})
B3	5.49 ± 1.06	2.89 ± 0.16	0.36 ± 0.05	0.01 ± 0.01	0.21 ± 0.03	121 ± 26.9	2.8 ± 0.5	2.7 ± 0.5	3.6 ± 0.4	3.38 ± 0.80
	4.70–7.31	2.75–3.17	0.31–0.44	−0.01 – 0.03	0.17–0.26	93.2–157	1.9–3.6	1.9–3.4	3.2–4.1	2.44–4.21
B13	0.69 ± 0.24	0.87 ± 0.14	0.16 ± 0.03	0.12 ± 0.02	0.28 ± 0.06	23.2 ± 0.80	6.3 ± 0.2	5.2 ± 0.5	18 ± 5.7	2.00 ± 0.99
	0.53–1.18	0.63–1.05	0.14–0.24	0.10–0.16	0.16–0.36	22.3–24.2	6.0–6.4	4.5–5.6	13–26	1.01–2.99
B14	0.03 ± 0.00	0.59 ± 0.01	0.09 ± 0.00	0.08 ± 0.00	0.25 ± 0.01	10.9 ± 3.50	7.8 ± 3.4	6.2 ± 0.7	8.0 ± 2.3	1.33 ± 0.35
	0.02–0.04	0.53–0.67	0.09–0.09	0.08–0.08	0.23–0.27	8.50–15.5	4.7–14	4.5–8.8	4.7–10	0.94–2.02
B15	1.82 ± 2.78	0.75 ± 0.25	0.19 ± 0.18	0.07 ± 0.01	0.19 ± 0.03	6.40 ± 1.40	14 ± 2.2	7.8 ± 1.0	38 ± 3.6	1.94 ± 0.37
	0.01–6.63	0.36–1.03	0.06–0.50	0.06–0.09	0.15–0.24	5.40–8.30	11–16	7.1–9.2	34–42	1.66–2.68
B16	1.15 ± 1.12	1.45 ± 0.74	0.23 ± 0.08	0.15 ± 0.06	0.16 ± 0.05	24.7 ± 9.10	8.6 ± 0.2	6.9 ± 0.1	19 ± 1.6	0.86 ± 0.18
	0.04–2.86	0.80–2.55	0.08–0.32	0.08–0.23	0.11–0.23	9.70–36.6	8.3–8.9	6.6–7.1	17–20	0.62–1.15
B17	2.02 ± 2.57	1.16 ± 0.47	0.32 ± 0.29	0.19 ± 0.14	0.25 ± 0.13	20.2 ± 22.8	17 ± 0.9	13 ± 0.3	24 ± 4.1	2.47 ± 0.22
	0.04–6.60	0.76–2.06	0.10–0.88	0.09–0.47	0.14–0.50	5.60–59.6	16–18	13–13	20–31	2.24–2.81

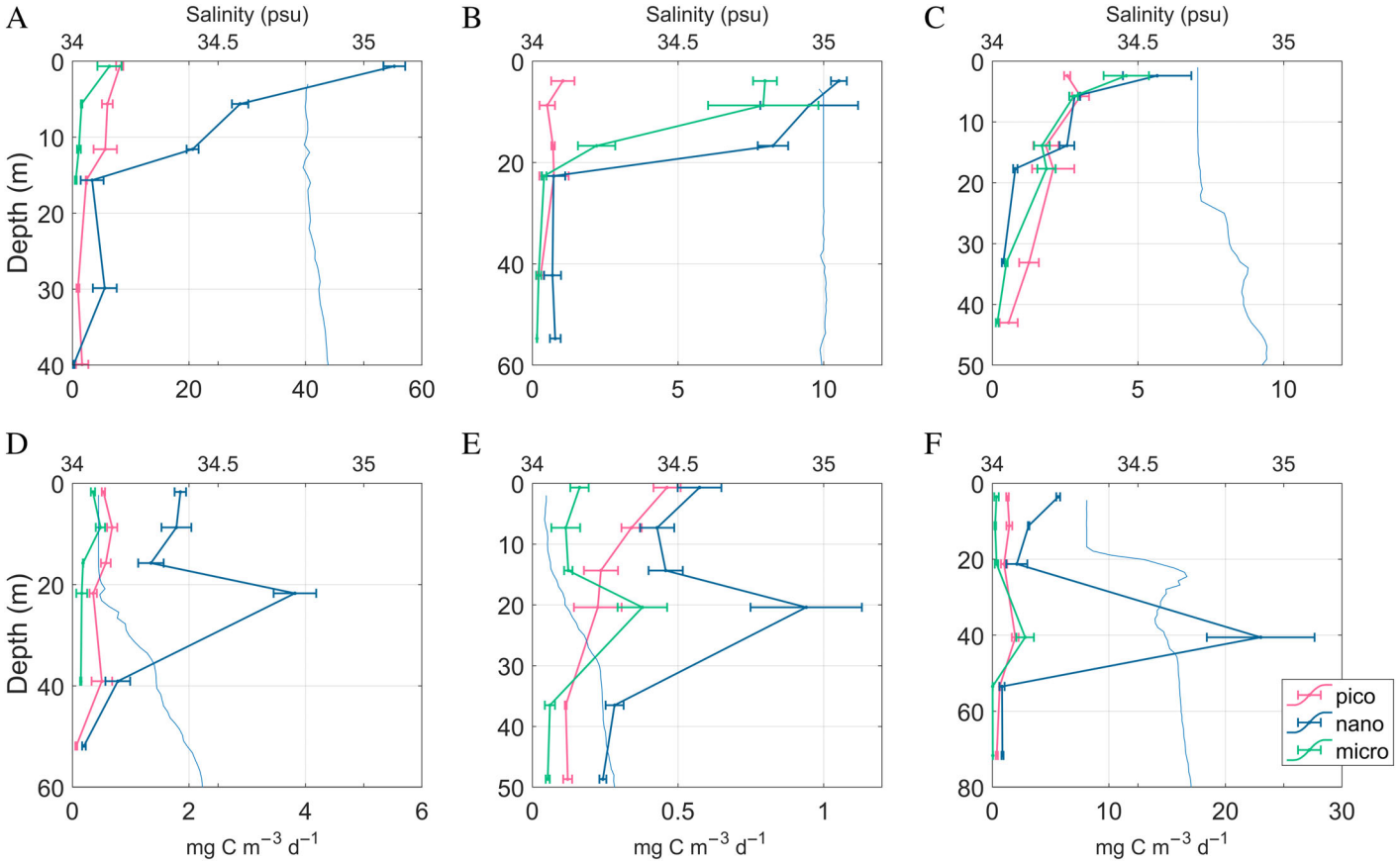

Fig 3. Size fractionated depth profiles of net primary production (pico < 2 μm, nano 2–20 μm, micro > 20 μm) and salinity (solid blue line) at Sta. (**A**) B3, (**B**), B13, (**C**) B14, (**D**) B15, (**E**) B16, and (**F**) B17. Note varied lower *x*-axis primary production scales and *y*-axis depth scales.

($p < 0.001$) with the environmental variables (Table 4), and again the temperature was part of every combination and showed strong latitudinal variation at these stations. Also, DIP concentration and its relative availability was part of the best correlated variables (Table 4), suggesting a more important role of DIP in forcing patterns of phytoplankton distribution in Atlantic waters alone.

Dissolved inorganic phosphorus uptake, dissolved organic phosphorus release, and alkaline phosphatase activity

DIP net uptake fluxes (determined using ^{33}P) were higher in the Atlantic section (8.50–158 nM d^{-1}) compared to the Arctic (5.40–59.6 nM d^{-1}; Table 2). An ANOVA test ($F = 5.36$, $p = 0.031$) revealed these differences between the Atlantic and Arctic water masses were statistically significant. The highest DIP uptake fluxes were at Sta. B3, which ranged between 93.2 and 157 nM d^{-1}. High rates of DIP uptake and PP at this station, were reflected in the low P* values (0.01 ± 0.04), suggesting ambient DIP was close to Redfield ratio. In contrast, the high *P. pouchetii* driven PP at B17 (Fig. 3F) corresponded to a high P* value of 0.47 at the PP peak (Fig. 6A), due to excess DIP compared to DIN.

Significant differences between the Atlantic and Arctic waters were also found for extracellular release of DOP (Fig. 6C; ANOVA, $F = 5.36$, $p = 0.03$). The fraction of assimilated DIP released as DOP was much greater in Arctic waters than Atlantic (Fig. 6B; Table 2). The lowest values were at Sta. B3, 3.2–4.1%, compared to 4.7–26% at the other Atlantic stations (B13 and B14) and 17–42% for the Arctic stations (Table 2).

The gross turnover time of DIP showed large variability, ranging from 1.9 to 13 d in surface waters above the nutricline depth (Figs. 6C, 7A), where high DIP uptake fluxes (8.5–158) in the Atlantic waters corresponded to faster gross turnover times (1.9–8.8) (Table 2). The most rapid average gross turnover time was at B3, 2.7 ± 0.5 d (Fig. 7A), despite having the greatest ambient DIP concentration of 0.36 ± 0.05 μM (Table 2; Fig. 2B). The ANOVA test revealed both net turnover ($F = 5.17$, $p = 0.03$) and gross turnover ($F = 11.29$, $p = 0.003$) were significantly different between Arctic and Atlantic waters. Differences between gross and net DIP turnover times can be attributed to the release of DOP (Fig. 7B). The relationship between the release of DOP and the gross turnover time (Fig. 8) shows a linear correlation coefficient of 0.77 ($R^2 = 0.593$). Although greater DOP release from cells results in

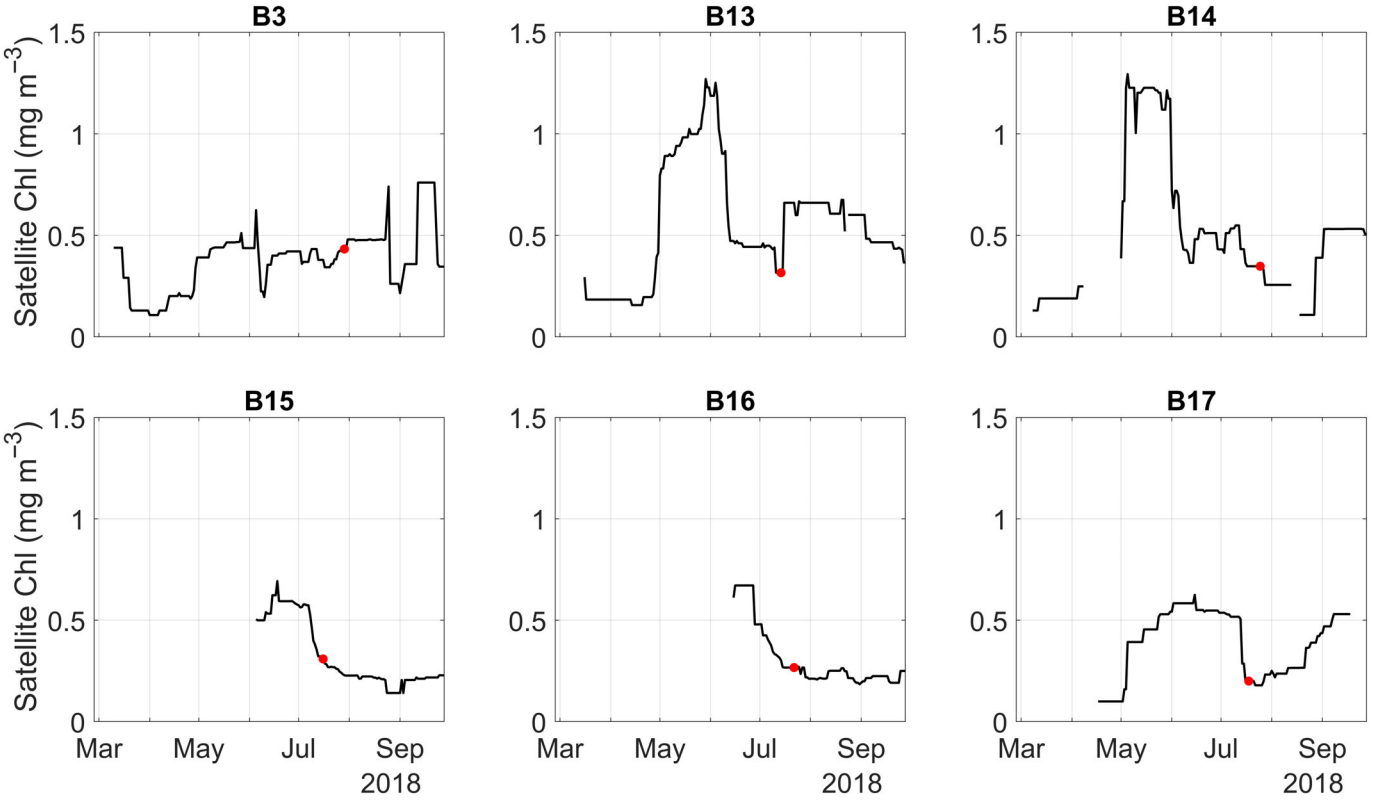

Fig 4. Satellite derived sea surface Chl *a* at each station from March–October 2018. Red circles indicate the day samples were collected during the cruise JR17007.

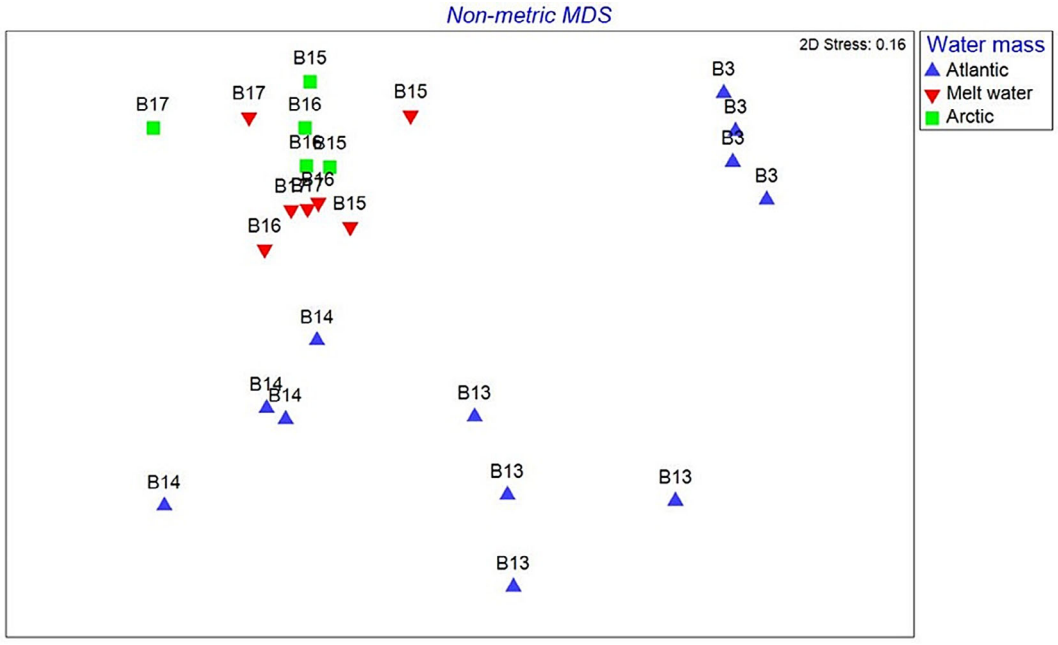

Fig 5. Nonmetric multidimensional scaling (NMDS) ordination of phytoplankton communities at each station. Based on a Bray–Curtis similarity matrix generated from fourth root transformed abundance data.

Table 3. Result of BEST analysis for all stations sampled ($p < 0.02$). The five best correlations between the multivariate patterns of phytoplankton community composition and environmental variables.

Spearman rank correlation	DIP	DIN	Silicate	P*	DOP	Salinity	Temperature
0.681			X				X
0.667	X		X	X		X	X
0.659			X			X	X
0.653		X	X	X		X	X
0.643	X		X	X			X

Table 4. Result of BEST analysis for the Atlantic stations only ($p < 0.001$). The five best correlations between the multivariate patterns of phytoplankton community composition and environmental variables.

Spearman rank correlation	DIP	DIN	Silicate	P*	DOP	Salinity	Temperature
0.789	X			X		X	X
0.766	X						X
0.764	X		X	X		X	X
0.763	X		X	X			X
0.762			X	X		X	X

faster gross turnover times compared to net turnover times (Fig. 7), DOP release and gross turnover time show a positive correlation, i.e., a high percentage of DOP release corresponds to slower turnover of the DIP pool.

AP activity ranged from 0.62 to 4.21 nM h^{-1} (Table 2). There was no significant difference between the Atlantic and Arctic stations (ANOVA, $F = 0.98$, $p = 0.331$). The highest rates were in the surface at Atlantic Sta. B3 (4.21 ± 0.08 nM hr^{-1}; Table 2) corresponding with the high PP (69.7 mg C m^3 d^{-1}; Fig. 3A) and high DIP uptake (96.92 nM d^{-1}), low percentage DOP release (4.0%) and a low P* (0.01) (Fig. 6). The lowest AP activity at Arctic Sta. B16 (0.86 ± 0.18 nM hr^{-1}; Table 2) was matched with very low rates of PP (41.4 mg C m^2 d^{-1}) along with low ambient DOP concentrations (0.16 ± 0.04 μM).

Discussion

There are distinct differences in nutrient stoichiometry between Arctic and Atlantic waters in the Barents Sea. Overlying melt water in the Arctic section results in enhanced vertical stratification and causes a subsurface peak in PP, with an apparent excess of DIP, denoted by relatively high P* values. At the Arctic stations silicate remained below the concentration limit (2 μM) required to support diatom dominated primary production (Egge and Aksnes 1992). Silicate limitation on PP has been reported for subarctic provinces, terminating diatom blooms (Krause et al. 2019). Our BEST analysis indicates that silicate and temperature are the dominant factors driving patterns in species distribution across both Atlantic and Arctic waters combined. It is likely that the early summer blooms indicated from satellite imagery results in silicate depletion in the surface layer, limiting diatom driven PP, resulting in phytoplankton species succession whereby *P. pouchetii* are the abundant species during the low nutrient summer period.

Nutrient concentrations in Atlantic waters varied between stations, with the highest ambient concentrations at the southern Sta. B3. This station is located toward the Barents Sea opening receiving Atlantic waters inflowing onto the shelf. As surface nutrient concentrations decrease moving from B3 to B14 so does the magnitude of PP and the species composition, shifting from autotrophic nanoplankton, e.g., phytoflagellates and *E. huxleyi*, to more mixotrophic communities dominated by dinoflagellates. Although DIP concentrations at B3 are relatively high (0.36 ± 0.05 μM), concentrations were close to, or below the Redfield ratio. In addition, the BEST analysis on Atlantic stations only, reveal a more significant role of DIP, its relative availability (P*), as well as the temperature in shaping the community structure.

The magnitude of PP varied greatly between the Arctic stations, yet the phytoplankton communities showed significant similarities, all being dominated by *P. pouchetii*. A subsurface peak in PP occurred at the 15% PAR depth for the three stations. At B17 this depth was situated at ~ 40 m, coinciding with much greater ambient nutrient availability with concomitant high PP; a factor of 5 and 15 greater than B15 and B16, respectively. At B15 and B16 the subsurface PP peak occurred at ~ 20 m, here nutrients, especially DIN were depleted, perhaps indicating post bloom more grazed conditions. DIN limitation is further apparent in the high P* values for these stations, showing a deficit of DIN relative to DIP. Nitrogen limited PP and subsurface chlorophyll maximums have

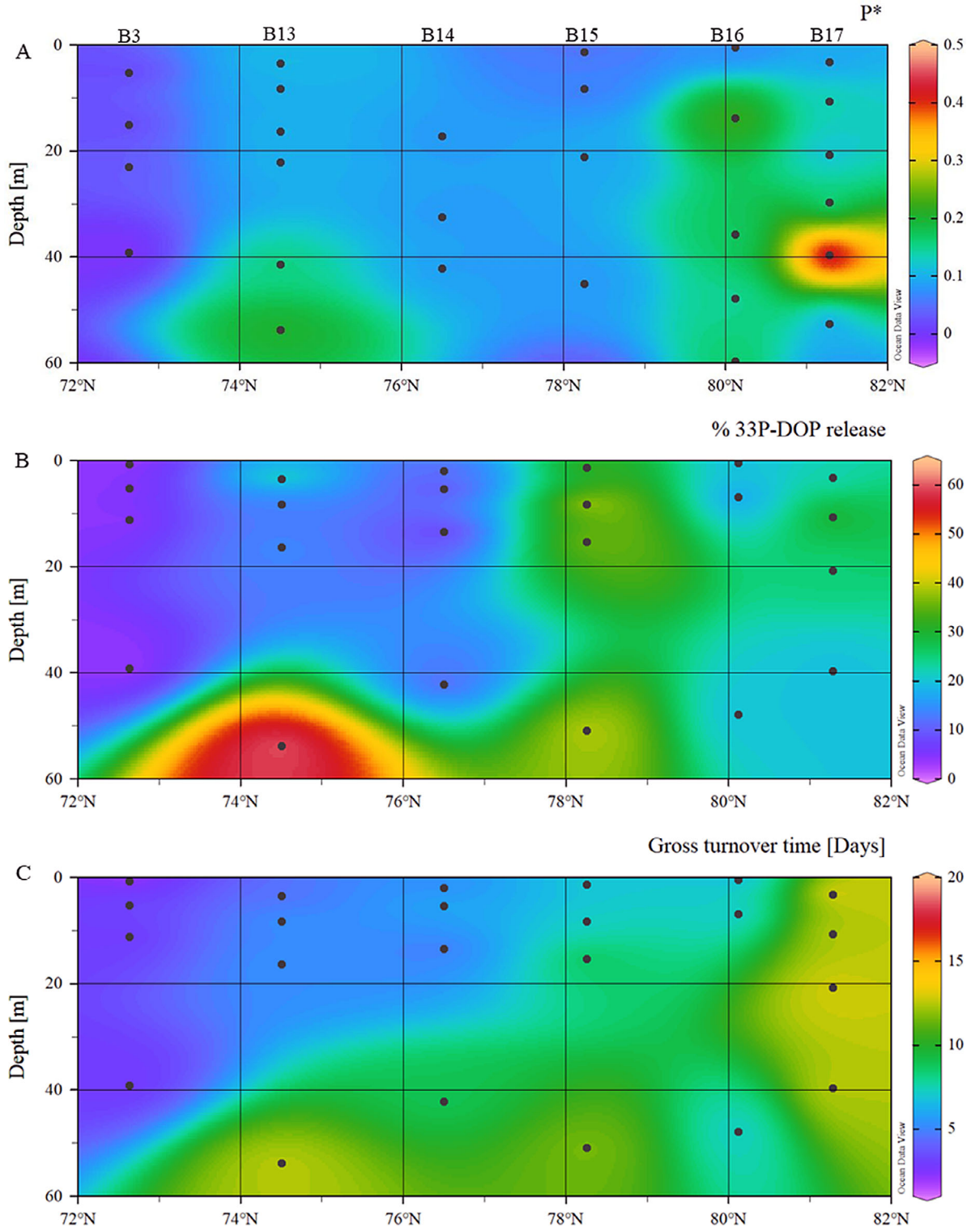

Fig 6. (**A**) Deviations of DIP concentration relative to Redfield ratio denoted as P*. (**B**) Percentage of incorporated ^{33}P-DIP released as DOP. (**C**) Gross turnover time of DIP.

previously been observed in Arctic waters surrounding the polar front region of the Barents Sea post spring bloom (Erga et al. 2014). When DIN is depleted, PP is predominately regenerated production, whereby phytoplankton growth is supported by the production of regenerated forms of N, such as ammonium and urea, by zooplankton grazing and

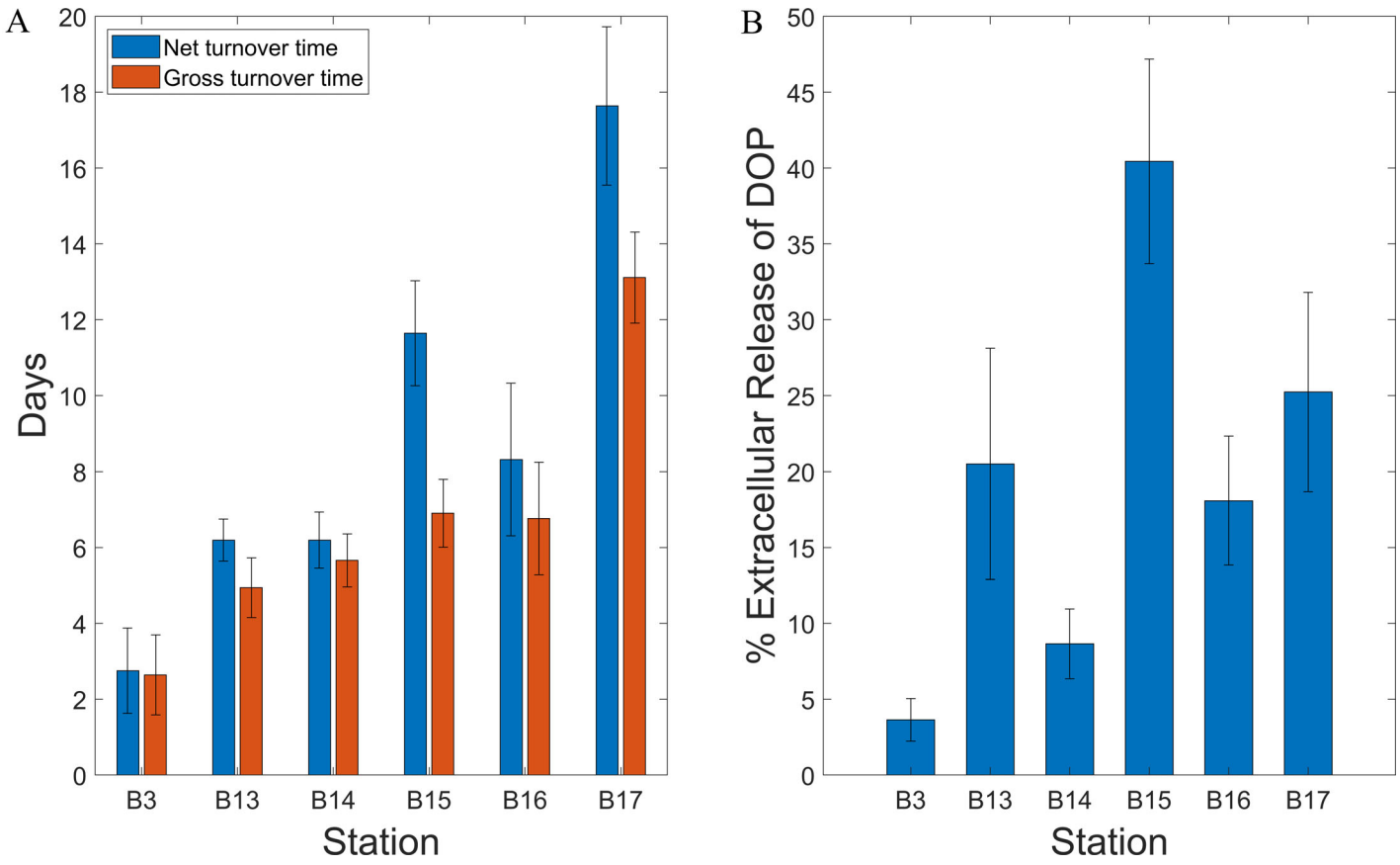

Fig 7. (**A**) Net and gross turnover time of ^{33}P-DIP in the upper water column (above nutricline depth). (**B**) Percentage of incorporated ^{33}P released as DOP.

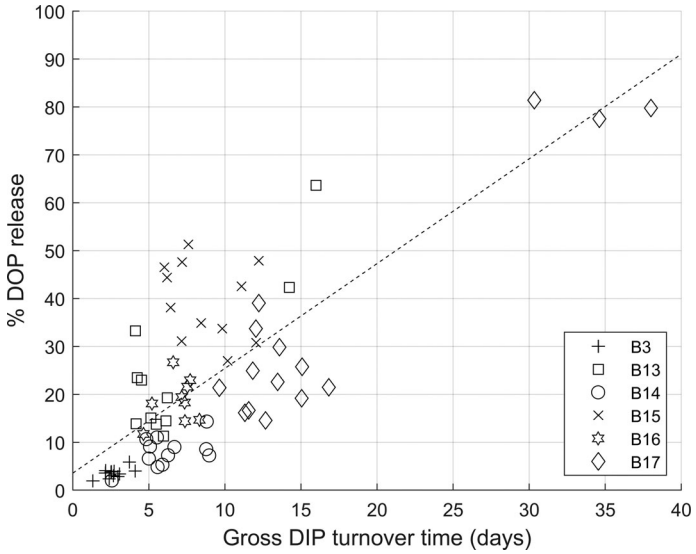

Fig 8. Relationship between extracellular release of DOP and gross turnover time of DIP. Linear correlation coefficient of 0.77 (R^2 = 0.593).

degradation of organic matter by heterotrophic bacteria. Ammonium and urea uptake have shown to account for 75–93% of total N uptake during the Barents Sea summer (Kristiansen et al. 1994). Unfortunately no ammonium and urea data was available for this study. However, it is likely that the rate of N regeneration is a key factor explaining the differences in PP between Arctic stations e.g., B15 and B16 where DIN was depleted at the subsurface PP peak for both sites but PP was 2.8 times greater at B15 compared to B16. At Sta. B17, the more transparent waters (the 1% PAR depth was ~ 70 m compared to ~ 50 m for B15 and B16) allow for phytoplankton to occur deeper in the nutricline, with greater ambient DIN concentrations, supporting much higher rates of PP.

Differences in DIP availability and phytoplankton P requirements, from Atlantic to Arctic waters are apparent in the turnover time of the DIP pool. Rather than comparing pool sizes and uptake rates alone, turnover time considers both, providing additional insight into the biogeochemical dynamics. Rapid biological uptake results in short turnover times (hours or days), while longer turnover times (weeks or months) implies lower cellular requirements or less bioavailability (Benitez-Nelson 2000). In general, the DIP turnover times we observed are consistent with that of open ocean systems ranging between days and weeks (Eppley et al. 1973; Harrison et al. 1977; Perry and Eppley 1981; Harrison 1983; Canellas et al. 2000; Sohm and Capone 2010). However, the

most rapid net turnover times observed in the southern Barents Sea at Sta. B3 (2.8 ± 0.5 d) could suggest that the phytoplankton communities are close to, or moving toward P deficiency.

Along with the shortest turnover time, we observed high P retention at Sta. B3 (expressed as a low fraction of assimilated DIP released as DOP). Here the average release of DOP is remarkably low (3.6 ± 0.4%), compared to all other stations (21 ± 9.7%) despite relatively high ambient DIP at Sta. B3 (0.36 ± 0.05 μM). This low extracellular release of DOP is comparable to summer time measurements (2–11%) in the Celtic shelf sea, whereby the planktonic community exhibited highly efficient P uptake and retention under low DIP conditions with ambient DIP concentrations ranging from 0.05 to 0.09 μM (Poulton et al. 2019). Furthermore, *E. huxleyi* was among the dominant phytoplankton species at B3, and it is known to have a large internal DIP pool, allowing them to proliferate in low DIP conditions (Riegman et al. 2000).

The portion of DIP assimilated and then released as DOP was significantly greater at the Arctic stations where the phytoplankton communities were comprised mainly of *P. pouchetii*, compared to the Atlantic stations with no *P. pouchetii* present. Previous field studies have observed high concentrations of dissolved organic carbon, dissolved carbohydrates and dissolved organic nitrogen during *Phaeocystis* blooms (Eberlein et al. 1985; Billen and Fontigny 1987). The life cycle of *P. pouchetii* has two main phases; solitary cells and colonial cells which are embedded in a matrix formed of mucoploysaccharides and heteropolysaccharies (Alderkamp et al. 2007). These carbon rich compounds can account for up to 90% of the total *Phaeocystis* biomass (Rousseau et al. 1990) resulting in high C/P and C/N ratios of organic matter produced by *Phaeocystis*. Hence, the higher rates of DOP release we observed in association with *Phaeocystis* communities are unlikely to be exclusively caused by these cells excreting colony mucus.

Alternatively, DOP release can result from herbivorous grazing and viral lysis where the labile cell contents are released as dissolved organic matter comprised of P rich compounds including phospholipids, nucleic acids and metabolic intermediates such as adenosine triphosphate. Unfortunately, there were no estimates of grazing rates during the current study. Despite a considerable amount of research there is still much uncertainty on the extent to which grazing pressure causes *Phaeocystis* mortality (Verity et al. 2007). The occurrence of *P. pouchetii* has previously been reported alongside low or insignificant herbivory rates (Calbet et al. 2011; Gifford et al. 1995; Saiz et al. 2013; Stoecker et al. 2015). Grazing dilution experiments conducted in Disko Bay, West Greenland, revealed a negative correlation between *Phaeocystis* spp. abundance and bulk grazing rate (Menden-Deuer et al. 2018). The authors hypothesized that this was likely a result of secondary metabolites, specifically polyunsaturated aldehydes, released by *Phaeocystis* which act as cytotoxic grazing deterrents (Franze et al. 2018; Menden-Deuer et al. 2018). In addition, the size of the colonies and the colony mucus has been hypothesized to provide mechanical protection and disrupt feeding by zooplankton (Kamermans 1994; Weisse et al. 1994). Despite this, large copepods including *Calanus* spp. are able to feed on *P. pouchetii* colonies (Nejstgaard et al. 2007). In the Barents Sea, *Calanus* spp. account for ~ 80% of the mesozooplankton biomass (Aarflot et al. 2018). Hence, the higher rates of DOP release we observed among *Phaeocystis* communities, could to be the consequence of grazing pressure from larger copepod species such as *Calanus* spp. which, through sloppy feeding and leakage from fecal pellets release phytoplankton derived organic phosphorus to the dissolved pool.

Viral lysis is also a major cause of mortality during *Phaeocystis* blooms (Brussaard et al. 1995, 1996, 2005). Culture experiments have shown that within 3 d, the entire *P. pouchetii* carbon biomass gets released as DOC due to viral lysis, compared to ~ 20% in control cultures with no virus present (Bratbak et al. 1998*a*). The host–virus system of *P. pouchetii* has a lytic cycle of 12–18 h (Jacobsen et al. 1996) and during most of the lytic cycle, primary production can continue (Bratbak et al. 1998*b*). Indicating that the 24 h incubations used in the present study could have undergone at least one, if not two lytic cycles, while infected cells were still metabolically active; assimilating DIP before cell lysis and the release of DOP. The correlation we observed between gross turnover time and the release of DOP could therefore be attributed to efficient P uptake and retention by the phytoplankton communities at the Atlantic stations (especially B3) and lower P requirements combined with a higher release of DOP via a combination of exudation, grazing and viral lysis at the Arctic stations (where *P. pouchetii* dominated phytoplankton communities).

AP activity remained relatively low, and within ranges previously reported for Atlantic and Arctic waters in the Fram Strait; 0–47.8 nM h^{-1} (Sala et al. 2010).To our knowledge there have been no previously published measurements of APA activity for the Barents Sea. The highest average value (3.38 ± 0.80 nM h^{-1}) recorded at the surface of Sta. B3 coincided with the high primary production, fast DIP turnover and low release of DOP. Combined, this could suggest DOP is being utilized as an alternative P source by members of the phytoplankton community. Here, *E. huxleyi* was present in relatively high abundance and is known to synthesize AP, under DIP limited conditions (Riegman et al. 2000). However, we found no significant difference in AP activity between Atlantic and Arctic stations. In addition, we are unable to attribute AP activity to either the phytoplankton or bacterioplankton communities based on the bulk activity method used. Therefore, it is likely that the DIP concentrations we measured were above the threshold required to stimulate high AP activity in response to P stress.

The prevalence of *E. huxleyi* in the southern Barents Sea is now a common phenomenon during the summer months

(Oziel et al. 2017). We observed the occurrence of *E. huxleyi* to be restricted to temperatures above ~ 6°C. This is consistent with satellite observations, where a Gaussian distribution of coccolithophore abundance centered around 8°C has been reported for this region (Signorini and McClain 2009). Our results indicate that the *E. huxleyi* dominated phytoplankton communities occurring in the warmer Atlantic waters likely have greater P requirements than that of Arctic phytoplankton communities. This results in a more rapid turnover and greater retention of assimilated DIP compared to Arctic phytoplankton assemblages. If the "Atlantification" of the Barents Sea shelf continues to intensify, the region may experience much faster and tighter cycling of phosphorus associated with the Atlantic phytoplankton communities, and ultimately become more P limited.

References

Aarflot, J. M., H. R. Skjoldal, P. Dalpadado, and M. Skern-Mauritzen. 2018. Contribution of Calanus species to the mesozooplankton biomass in the Barents Sea. ICES J. Mar. Sci. **75**: 2342–2354. doi: 10.1093/icesjms/fsx221

Alderkamp, A. C., A. G. J. Buma, and M. van Rijssel. 2007. The carbohydrates of Phaeocystis and their degradation in the microbial food web. Biogeochemistry **83**: 99–118. doi: 10.1007/s10533-007-9078-2

Arrigo, K. R., and G. L. van Dijken. 2015. Continued increases in Arctic Ocean primary production. Prog. Oceanogr. **136**: 60–70. doi: 10.1016/j.pocean.2015.05.002

Behrenfeld, M. J., et al. 2006. Climate-driven trends in contemporary ocean productivity. Nature **444**: 752–755. doi: 10.1038/nature05317

Benitez-Nelson, C. R. 2000. The biogeochemical cycling of phosphorus in marine systems. Earth Sci. Rev. **51**: 109–135. doi: 10.1016/S0012-8252(00)00018-0

Billen, G., and A. Fontigny. 1987. Dynamics of a Phaeocystis-dominated spring bloom in Belgian coastal waters. 2. Bacterioplankton dynamics. Mar. Ecol. Prog. Ser. **37**: 249–257. doi: http://www.jstor.org/stable/24824699

Bjorkman, K., and D. M. Karl. 1994. Bioavailability of inorganic and organic phosphorus-compounds to natural assemblages of microorganisms in hawaiian coastal waters. Mar. Ecol. Prog. Ser. **111**: 265–273. doi: http://www.jstor.org/stable/24849565

Bjorkman, K., A. L. Thomson-Bulldis, and D. M. Karl. 2000. Phosphorus dynamics in the North Pacific subtropical gyre. Aquat. Microb. Ecol. **22**: 185–198. doi: https://www.int-res.com/abstracts/ame/v22/n2/p185-198/

Bratbak, G., A. Jacobsen, and M. Heldal. 1998*a*. Viral lysis of *Phaeocystis pouchetii* and bacterial secondary production. Aquat. Microb. Ecol. **16**: 11–16. doi: 10.3354/ame016011

Bratbak, G., A. Jacobsen, M. Heldal, K. Nagasaki, and F. Thingstad. 1998*b*. Virus production in *Phaeocystis pouchetii* and its relation to host cell growth and nutrition. Aquat. Microb. Ecol. **16**: 1–9. doi: 10.3354/ame016001

Brussaard, C. P. D., and others. 1995. Effects of grazing, sedimentation and phytoplankton cell-lysis on the structure of a coastal pelagic food-web. Mar. Ecol. Prog. Ser. **123**: 259–271. doi: 10.3354/meps123259

Brussaard, C. P. D., G. J. Gast, F. C. vanDuyl, and R. Riegman. 1996. Impact of phytoplankton bloom magnitude on a pelagic microbial food web. Mar. Ecol. Prog. Ser. **144**: 211–221. doi: 10.3354/meps144211

Brussaard, C. P. D., B. Kuipers, and M. J. W. Veldhuis. 2005. A mesocosm study of *Phaeocystis globosa* population dynamics—1. Regulatory role of viruses in bloom. Harmful Algae **4**(5): 859–874. doi: 10.1016/j.hal.2004.12.015

Calbet, A., E. Saiz, R. Almeda, J. I. Movilla, and M. Alcaraz. 2011. Low microzooplankton grazing rates in the Arctic Ocean during a *Phaeocystis pouchetii* bloom (summer 2007): Fact or artifact of the dilution technique? J. Plankton Res. **33**: 687–701. doi: 10.1093/plankt/fbq142

Canellas, M., S. Agusti, and C. M. Duarte. 2000. Latitudinal variability in phosphate uptake in the Central Atlantic. Mar. Ecol. Prog. Ser. **194**: 283–294. doi: https://www.jstor.org/stable/24855672

Carmack, E., D. Barber, J. Christensen, R. Macdonald, B. Rudels, and E. Sakshaug. 2006. Climate variability and physical forcing of the food webs and the carbon budget on panarctic shelves. Prog. Oceanogr. **71**: 145–181. doi: 10.1016/j.pocean.2006.10.005

Clarke, K. R. 1993. Nonparametric multivariate analyses of changes in community structure. Aust. J. Ecol. **18**: 117–143. doi: 10.1111/j.1442-9993.1993.tb00438.x

Clarke, K. R., and M. Ainsworth. 1993. A method of linking multivariate community structure to environmental variables. Mar. Ecol. Prog. Ser. **92**: 205–219. doi: 10.3354/meps092205

Clarke, K. R., and R. H. Green. 1988. Statistical design and analysis for a biological effects study. Mar. Ecol. Prog. Ser. **46**: 213–226. doi: 10.3354/meps046213

Davis, C. E., and C. Mahaffey. 2017. Elevated alkaline phosphatase activity in a phosphate-replete environment: Influence of sinking particles. Limnol. Oceanogr. **62**: 2389–2403. doi: 10.1002/lno.10572

Degerlund, M., and H. C. Eilertsen. 2010. Main species characteristics of phytoplankton spring blooms in NE Atlantic and Arctic waters (68-80A degrees N). Estuaries Coasts **33**: 242–269. doi: https://www.jstor.org/stable/40663692

Deutsch, C., and T. Weber. 2012. Nutrient ratios as a tracer and driver of ocean biogeochemistry, p. 113. *In* C. A. Carlson and S. J. Giovannoni–141. [eds.], Annual review of marine science, v. **4**. Annual Reviews. doi: https://www.annualreviews.org/doi/abs/10.1146/annurev-marine-120709-142821

Donlon, C. J., M. Martin, J. Stark, J. Roberts-Jones, E. Fiedler, and W. Wimmer. 2012. The operational sea surface

temperature and sea ice analysis (OSTIA) system. Remote Sens. Environ. **116**: 140–158. doi: 10.1016/j.rse.2010.10.017

Eberlein, K., M. T. Leal, K. D. Hammer, and W. Hickel. 1985. Dissolved organic-substances during a *Phaeocystis pouchetii* bloom in the German Bight (North-Sea). Mar. Biol. **89**: 311–316. doi: 10.1007/BF00393665

Edwards, K. F., M. K. Thomas, C. A. Klausmeier, and E. Litchman. 2012. Allometric scaling and taxonomic variation in nutrient utilization traits and maximum growth rate of phytoplankton. Limnol. Oceanogr. **57**: 554–566. doi: 10.4319/lo.2012.57.2.0554

Egge, J. K., and D. L. Aksnes. 1992. Silicate as regulating nutrient in phytoplankton competition. Mar. Ecol. Prog. Ser. **83**: 281–289. doi: https://www.jstor.org/stable/24827612

Eppley, R. W., E. H. Renger, E. L. Venrick, and M. M. Mullin. 1973. Study of plankton dynamics and nutrient cycling in central gyre of North Pacific ocean. Limnol. Oceanogr. **18**: 534–551. doi: 10.4319/lo.1973.18.4.0534

Erga, S. R., N. Ssebiyonga, B. Hamre, O. Frette, F. Rey, and K. Drinkwater. 2014. Nutrients and phytoplankton biomass distribution and activity at the Barents Sea polar front during summer near Hopen and Storbanken. J. Mar. Syst. **130**: 181–192. doi: 10.1016/j.jmarsys.2012.12.008

Falkowski, P. G., R. T. Barber, and V. Smetacek. 1998. Biogeochemical controls and feedbacks on ocean primary production. Science **281**: 200–206. doi: https://science.sciencemag.org/content/sci/281/5374/200.full.pdf

Franze, G., J. J. Pierson, D. K. Stoecker, and P. J. Lavrentyev. 2018. Diatom-produced allelochemicals trigger trophic cascades in the planktonic food web. Limnol. Oceanogr. **63**: 1093–1108. doi: 10.1002/lno.10756

Gifford, D. J., L. M. Fessenden, P. R. Garrahan, and E. Martin. 1995. Grazing by microzooplankton and mesozooplankton in the high-latitude North-Atlantic Ocean—spring versus summer dynamics. J. Geophys. Res. Oceans **100**: 6665–6675. doi: 10.1029/94JC00983

Harrison, W. G. 1983. Uptake and recycling of soluble reactive phosphorus by marine microplankton. Mar. Ecol. Prog. Ser. **10**: 127–135. doi: https://www.jstor.org/stable/24815185

Harrison, W. G., F. Azam, E. H. Renger, and R. W. Eppley. 1977. Some experiments on phosphate assimilation by coastal marine plankton. Mar. Biol. **40**: 9–18. doi: 10.1007/BF00390622

Hecky, R. E., and P. Kilham. 1988. Nutrient limitation of phytoplankton in fresh-water and marine environments—a review of recent-evidence on the effects of enrichment. Limnol. Oceanogr. **33**: 796–822. doi: 10.4319/lo.1988.33.4part2.0796

Hegseth, E. N., and A. Sundfjord. 2008. Intrusion and blooming of Atlantic phytoplankton species in the high Arctic. J. Mar. Syst. **74**: 108–119. doi: 10.1016/j.jmarsys.2007.11.011

Hoppe, H. G. 1983. Significance of exoenzymatic activities in the ecology of brackish water—measurements by means of methylumbelliferyl-substrates. Mar. Ecol. Prog. Ser. **11**: 299–308. doi: https://www.jstor.org/stable/44634717

Hovland, E. K., et al. 2014. Optical impact of an *Emiliania huxleyi* bloom in the frontal region of the Barents Sea. J. Mar. Syst. **130**: 228–240. doi: 10.1016/j.jmarsys.2012.07.002

Jacobsen, A., G. Bratbak, and M. Heldal. 1996. Isolation and characterization of a virus infecting *Phaeocystis pouchetii* (Prymnesiophyceae). J. Phycol. **32**: 923–927. doi: 10.1111/j.0022-3646.1996.00923.x

Joint, I., and A. Pomroy. 1993. Phytoplankton biomass and production in the southern North-Sea. Mar. Ecol. Prog. Ser. **99**: 169–182. doi: https://www.jstor.org/stable/24837760

Kamermans, P. 1994. Nutritional-value of solitary cells and colonies of *Phaeocystis*-sp for the bivalve Macoma-balthica (l). Ophelia **39**: 35–44. doi: 10.1080/00785326.1994.10429900

Karl, D. M. 2014. Microbially mediated transformations of phosphorus in the sea: New views of an old cycle, p. 279–337. *In* C. A. Carlson and S. J. Giovannoni [eds.], Annual review of marine science, v. **6**. Annual Reviews. doi: 10.1146/annurev-marine-010213-135046

Karl, D. M., and K. M. Björkman. 2015. Dynamics of dissolved organic phosphorus, p. 233–334. *In* D. A. Hansell and C. A. Carlson [eds.], Biogeochemistry of marine dissolved organic matter, 2nd ed. Academic Press. doi: 10.1016/B978-0-12-405940-5.00005-4

Krause, J. W., et al. 2019. Silicic acid limitation drives bloom termination and potential carbon sequestration in an Arctic bloom. Sci. Rep. **9**: 8149. doi: 10.1038/s41598-019-44587-4

Kristiansen, S., T. Farbrot, and P. A. Wheeler. 1994. Nitrogen cycling in the barents sea—seasonal dynamics of new and regenerated production in the marginal ice-zone. Limnol. Oceanogr. **39**: 1630–1642. doi: 10.4319/lo.1994.39.7.1630

Labry, C., and others. 2016. High alkaline phosphatase activity in phosphate replete waters: The case of two macrotidal estuaries. Limnol. Oceanogr. **61**: 1513–1529. doi: 10.1002/lno.10315

Lessard, E. J., A. Merico, and T. Tyrrell. 2005. Nitrate : Phosphate ratios and *Emiliania huxleyi* blooms. Limnol. Oceanogr. **50**: 1020–1024. doi: 10.4319/lo.2005.50.3.1020

Lind, S., R. B. Ingvaldsen, and T. Furevik. 2018. Arctic warming hotspot in the northern Barents Sea linked to declining sea-ice import. Nat. Clim. Change **8**: 634–639. doi: 10.1038/s41558-018-0205-y

Loeng, H., V. Ozhigin, and B. Adlandsvik. 1997. Water fluxes through the Barents Sea. ICES J. Mar. Sci. **54**: 310–317. doi: 10.1006/jmsc.1996.0165

Lomas, M. W., and others. 2010. Sargasso Sea phosphorus biogeochemistry: An important role for dissolved organic phosphorus (DOP). Biogeosciences **7**: 695–710. doi: 10.5194/bg-7-695-2010

Lomas, M. W., J. A. Bonachela, S. A. Levin, and A. C. Martiny. 2014. Impact of ocean phytoplankton diversity on phosphate uptake. Proc. Natl. Acad. Sci. U. S. A. **111**: 17540–17545. doi: 10.1073/pnas.1420760111

Luchetta, A., M. Lipizer, and G. Socal. 2000. Temporal evolution of primary production in the Central Barents Sea. J. Mar. Syst. **27**: 177–119. doi: 10.1016/S0924-7963(00)00066-X

Mahaffey, C., S. Reynolds, C. E. Davis, and M. C. Lohan. 2014. Alkaline phosphatase activity in the subtropical ocean: Insights from nutrient, dust and trace metal addition experiments. Front. Mar. Sci. **1**: 73. doi: 10.3389/fmars.2014.00073

Menden-Deuer, S., C. Lawrence, and G. Franze. 2018. Herbivorous protist growth and grazing rates at in situ and artificially elevated temperatures during an Arctic phytoplankton spring bloom. Peerj **6**: e5264. doi: 10.7717/peerj.5264

Menzel, D. W., and N. Corwin. 1965. The measurement of total phosphorus in seawater based on the liberation of organically bound fractions by persulfate oxidation. Limnol. Oceanogr. **10**: 280–282. doi: 10.4319/lo.1965.10.2.0280

Moutin, T., and others. 2002. Does competition for nanomolar phosphate supply explain the predominance of the cyanobacterium Synechococcus? Limnol. Oceanogr. **47**: 1562–1567. doi: 10.4319/lo.2002.47.5.1562

Nejstgaard, J. C., and others. 2007. Zooplankton grazing on Phaeocystis: A quantitative review and future challenges. Biogeochemistry **83**: 147–172. doi: 10.1007/s10533-007-9098-y

Neukermans, G., L. Oziel, and M. Babin. 2018. Increased intrusion of warming Atlantic water leads to rapid expansion of temperate phytoplankton in the Arctic. Glob. Chang. Biol. **24**: 2545–2553. doi: 10.1111/gcb.14075

Oziel, L., and others. 2017. Role for Atlantic inflows and sea ice loss on shifting phytoplankton blooms in the Barents Sea. J. Geophys. Res.: Oceans **122**: 5121–5139. doi: 10.1002/2016JC012582

Oziel, L., J. Sirven, and J. C. Gascard. 2016. The Barents Sea frontal zones and water masses variability (1980-2011). Ocean Sci. **12**: 169–184. doi: 10.5194/os-12-169-2016

Perry, M. J., and R. W. Eppley. 1981. Phosphate-uptake by phytoplankton in the central North Pacific-Ocean. Deep-Sea Res. Pt. A: Oceanogr. Res. Pap. **28**: 39–49. doi: 10.1016/0198-0149(81)90109-6

Poulton, A. J., and others. 2019. Seasonal phosphorus and carbon dynamics in a temperate shelf sea (Celtic Sea). Prog. Oceanogr. **177**: 15. doi: 10.1016/j.pocean.2017.11.001

Rees, A. P., S. B. Hope, C. E. Widdicombe, J. L. Dixon, E. M. S. Woodward, and M. F. Fitzsimons. 2009. Alkaline phosphatase activity in the western English Channel: Elevations induced by high summertime rainfall. Estuarine Coast. Shelf Sci. **81**: 569–574. doi: 10.1016/j.ecss.2008.12.005

Ridal, J. J., and R. M. Moore. 1990. A reexamination of the measurement of dissolved organic phosphorus in seawater. Mar. Chem. **29**: 19–31. doi: 10.1016/0304-4203(90)90003-U

Riegman, R., W. Stolte, A. A. M. Noordeloos, and D. Slezak. 2000. Nutrient uptake, and alkaline phosphate (EC 3:1:3:1) activity of *Emiliania huxleyi* (Prymnesiophyceae) during growth under N and P limitation in continuous cultures. J. Phycol. **36**: 87–96. doi: 10.1046/j.1529-8817.2000.99023.x

Rousseau, V., S. Mathot, and C. Lancelot. 1990. Calculating carbon biomass of *Phaeocystis* sp from microscopic observations. Mar. Biol. **107**: 305–314. doi: 10.1007/BF01319830

Saiz, E., and others. 2013. Zooplankton distribution and feeding in the Arctic Ocean during a *Phaeocystis pouchetii* bloom. Deep-Sea Res. Pt. I: Oceanogr. Res. Pap. **72**: 17–33. doi: 10.1016/j.dsr.2012.10.003

Sakshaug, E., and H. R. Skjoldal. 1989. Life at the ice edge. Ambio **18**: 60–67. doi: https://www.jstor.org/stable/4313526

Sakshaug, E., A. Bjorge, B. Gulliksen, H. Loeng, and F. Mehlum. 1994. Structure, biomass distribution, and energetics of the pelagic ecosystem in the barents sea—a synopsis. Polar Biol. **14**: 405–411. doi: 10.1007/BF00240261

Sala, M. M., J. M. Arrieta, J. A. Boras, C. M. Duarte, and D. Vaque. 2010. The impact of ice melting on bacterioplankton in the Arctic Ocean. Polar Biol. **33**: 1683–1694. doi: 10.1007/s00300-010-0808-x

Sebastian, M., J. Aristegui, M. F. Montero, and F. X. Niell. 2004. Kinetics of alkaline phosphatase activity, and effect of phosphate enrichment: A case study in the NW African upwelling region. Mar. Ecol. Prog. Ser. **270**: 1–13. doi: https://www.int-res.com/abstracts/meps/v270/p1-13/

Signorini, S. R., and C. R. McClain. 2009. Environmental factors controlling the Barents Sea spring-summer phytoplankton blooms. Geophys. Res. Lett. **36**: 10. doi: 10.1029/2009GL037695

Smyth, T. J., T. Tyrrell, and B. Tarrant. 2004. Time series of coccolithophore activity in the Barents Sea, from twenty years of satellite imagery. Geophys. Res. Lett. **31**: 11. doi: 10.1029/2004GL019735

Sohm, J. A., and D. G. Capone. 2010. Zonal differences in phosphorus pools, turnover and deficiency across the tropical North Atlantic Ocean. Glob. Biogeochem. Cycles **24**: 2. doi: 10.1029/2008GB003414

Stoecker, D. K., et al. 2015. Underestimation of microzooplankton grazing in dilution experiments due to inhibition of phytoplankton growth. Limnol. Oceanogr. **60**: 1426–1438. doi: 10.1002/lno.10106

Tanaka, T., F. Rassoulzadegan, and T. F. Thingstad. 2003. Measurements of phosphate affinity constants and phosphorus release rates from the microbial food web in Villefranche Bay, northwestern Mediterranean. Limnol. Oceanogr. **48**: 1150–1160. doi: 10.4319/lo.2003.48.3.1150

Thingstad, T. F., and others. 2005. Nature of phosphorus limitation in the ultraoligotrophic eastern Mediterranean. Science **309**(5737): 1068–1071. doi: 10.1126/science.1112632

Thingstad, T. F., U. L. Zweifel, and F. Rassoulzadegan. 1998. P limitation of heterotrophic bacteria and phytoplankton in the Northwest Mediterranean. Limnol. Oceanogr. **43**: 88–94. doi: 10.4319/lo.1998.43.1.0088

Thomson-Bulldis, A., and D. Karl. 1998. Application of a novel method for phosphorus determinations in the oligotrophic North Pacific Ocean. Limnol. Oceanogr. **43**: 1565–1577. doi: 10.4319/lo.1998.43.7.1565

Torres-Valdes, S., et al. 2009. Distribution of dissolved organic nutrients and their effect on export production over the Atlantic Ocean. Glob. Biogeochem. Cycles **23**: 4. doi: 10.1029/2008GB003389

Tremblay, J. E., and J. Gagnon. 2009. The effects of irradiance and nutrient supply on the productivity of Arctic waters: A perspective on climate change, p. 73–93. *In* J. C. J. Nihoul and A. G. Kostianoy [eds.], Influence of climate change on the changing Arctic and sub-Arctic conditions. NATO science for peace and security series C-environmental security. Springer. doi: 10.1007/978-1-4020-9460-6_7

Tyrrell, T. 1999. The relative influences of nitrogen and phosphorus on oceanic primary production. Nature **400**: 525–531. doi: 10.1038/22941

Tyrrell, T., and A. Merico. 2004. Emiliania huxleyi: Bloom observations and the conditions that induce them. Coccolithophores, (pp. 75–97). New York: Springer. doi: 10.1007/978-3-662-06278-4_4

Vage, K., et al. 2016. The Atlantic water boundary current in the Nansen Basin: Transport and mechanisms of lateral exchange. J. Geophys. Res.: Oceans **121**: 6946–6960. doi: 10.1002/2016JC011715

Verity, P. G., C. P. Brussaard, J. C. Nejstgaard, M. A. van Leeuwe, C. Lancelot, and L. K. Medlin. 2007. Current understanding of Phaeocystis ecology and biogeochemistry, and perspectives for future research. Biogeochemistry **83**: 311–330. doi: 10.1007/s10533-007-9090-6

Wassmann, P., and others. 2006. Food webs and carbon flux in the Barents Sea. Prog. Oceanogr. **71**: 232–287. doi: 10.1016/j.pocean.2006.10.003

Wassmann, P., T. Ratkova, I. Andreassen, M. Vernet, C. Pedersen, and F. Rey. 1999. Spring bloom development in the marginal ice zone and the Central Barents Sea. Mar. Ecol.: Pubblicazioni Della Stazione Zoologica Di Napoli I **20**: 321–346. doi: 10.1046/j.1439-0485.1999.2034081.x

Weisse, T., K. Tande, P. Verity, F. Hansen, and W. Gieskes. 1994. The trophic significance of Phaeocystis blooms. J. Mar. Syst. **5**: 67–79. doi: 10.1016/0924-7963(94)90017-5

Widdicombe, C. E., D. Eloire, D. Harbour, R. P. Harris, and P. J. Somerfield. 2010. Long-term phytoplankton community dynamics in the Western English Channel. J. Plankton Res. **32**: 643–655. doi: 10.1093/plankt/fbp127

Woodward, E. M. S., and A. P. Rees. 2001. Nutrient distributions in an anticyclonic eddy in the Northeast Atlantic Ocean, with reference to nanomolar ammonium concentrations. Deep-Sea Res. Pt. II: Top. Stud. Oceanogr. **48**: 775–793. doi: 10.1016/S0967-0645(00)00097-7

Wu, J. F., W. Sunda, E. A. Boyle, and D. M. Karl. 2000. Phosphate depletion in the western North Atlantic Ocean. Science **289**: 759–762. doi: https://science.sciencemag.org/content/sci/289/5480/759.full.pdf

Yoshimura, T. 2013. Appropriate bottles for storing seawater samples for dissolved organic phosphorus (DOP) analysis: A step toward the development of DOP reference materials. Limnol. Oceanogr.: Methods **11**: 239–246. doi: 10.4319/lom.2013.11.239

Acknowledgments

We thank Christian Maerz and members of the ChAOS project for allowing us to join the research cruise. We also thank Geoff Abbott and Mark Stevenson for providing frozen water samples for nutrient analysis. We would like to thank the crew of the *RRS James Clark Ross* for their work in facilitating the field campaign. This work was principally funded by the NERC GW4+ DTP grant (NE/L002434/1) and benefitted from alignment on fieldwork with both the NERC Discovery grant titled "Is bacterial DMS consumption dependent on methylamines in marine waters" (NE/R010382/1) and with the Changing Arctic Ocean Seafloor (ChAOS) project (NE/P006493/1), part of the Changing Arctic Ocean programme, funded by the UKRI Natural Environment Research Council (NERC). This work also substantially benefited from a successful application to the NERC Earth Observation Data Acquisition Analysis Service (NEODAAS) who supplied satellite remotely sensed products.

Conflict of interest

None declared.

Submitted 02 March 2020
Revised 03 July 2020
Accepted 20 August 2020

Associate editor: Ronnie Glud